Essential functions of ezrin in maintenance of cell shape and lamellipodial extension in normal and transformed fibroblasts

Richard F. Lamb*, Bradford W. Ozanne*, Christian Roy†, Lynn McGarry*, Christopher Stipp‡, Paul Mangeat† and Daniel G. Jay‡

Background: Changes in cell shape and motility are important manifestations of oncogenic transformation, but the mechanisms underlying these changes and key effector molecules in the cytoskeleton remain unknown. The Fos oncogene induces expression of ezrin, the founder member of the ezrin/radixin/moesin (ERM) protein family, but not expression of the related ERM proteins, suggesting that ezrin has a distinct role in cell transformation. ERM proteins have been suggested to link the plasma membrane to the actin-based cytoskeleton and are substrates and anchoring sites for a variety of protein kinases. Here, we examined the role of ezrin in cellular transformation.

Results: Fos-mediated transformation of Rat-1 fibroblasts resulted in an increased expression and hyperphosphorylation of ezrin, and a concomitant increased association of ezrin with the cortical cytoskeleton. We tagged ezrin with green fluorescent protein and examined its distribution in normal and Fos-transformed fibroblasts: ezrin was concentrated at the leading edge of extending pseudopodia of Fos-transformed Rat-1 cells, and was mainly cytosolic in normal Rat-1 cells. Functional ablation of ezrin by micro-CALI (chromophore-assisted laser inactivation) blocked plasma-membrane ruffling and motility of Fos-transformed fibroblasts. Ablation of ezrin in normal Rat-1 cells caused a marked collapse of the leading edge of the cell.

Conclusion: Ezrin plays an important role in pseudopodial extension in Fos-transformed Rat-1 fibroblasts, and maintains cell shape in normal Rat-1 cells. The increased expression, hyperphosphorylation and subcellular redistribution of ezrin upon fibroblast transformation coupled with its roles in cell shape and motility suggest a critical role for ezrin in oncogenic transformation.

Addresses: *Beatson Institute for Cancer Research, CRC Beatson Laboratories, Wolfson Laboratory for Molecular Pathology, Garscube Estate, Switchback Road, Bearsden, Glasgow G61 1BD, Scotland, UK. †Dynamique Moleculaire des Interactions Membranaires, CNRS UMR 5539, Universite Montpellier 2, CC 107, 34095 Montpellier Cedex 5, France. ‡ Department of Molecular and Cellular Biology, 16 Divinity Avenue, Harvard University, Cambridge, Massachusetts, 02138, USA.

Correspondence: Richard F. Lamb
E-mail: rlamb@ucl.ac.uk

Received: **19 May 1997**
Revised: **26 June 1997**
Accepted: **17 July 1997**

Published: **19 August 1997**

Current Biology 1997, 7:682–688
http://biomednet.com/elecref/0960982200700682

Background

The actin-based cytoskeleton plays a central role in cell motility and cortical morphogenesis, and is reorganized during cell transformation [1]. Ezrin, the founder member of the ezrin/radixin/moesin (ERM) family, has been proposed to function as a molecular linker, modulating cortical morphogenesis by tethering actin microfilaments to the plasma membrane [2,3]. Ezrin expression is increased during cellular transformation by Fos [4]; Fos family members heterodimerise with those of the Jun family to form AP-1 proteins, a group of transcription factors required for oncogenic transformation [5,6].

Recent evidence indicates that a major plasma-membrane ligand for ERM proteins might be the hyaluronan receptor CD44 [7]. We have shown previously that CD44 expression is regulated by AP-1 and that CD44 is required for the *in vitro* invasion of Fos-transformed Rat-1 fibroblasts into extracellular matrix [8,9]. These data suggested that ezrin might also play an important role in motility, but a precise role of ezrin in transformation remained unclear. In these studies, we examined ezrin phosphorylation, the association of ezrin with the plasma membrane and its effects on the cytoskeleton and cell dynamics. We also examined the consequences of the functional inactivation of ezrin in normal and Fos-transformed Rat-1 fibroblasts.

Results

Transformation by Fos induces ezrin hyperphosphorylation and relocalization

Stable transformation of Rat-1 cells by Fos led to increased ezrin expression ([4], Figure 1a) and hyperphosphorylation of ezrin (Figure 1b,c). Fos-induced transformation also caused a significant enrichment of ezrin associated with the cytoskeleton (Figure 1d,e); this enrichment did not occur in Fos-transformed Rat-1 cells that expressed a transactivation-defective dominant-negative inhibitor of AP-1 (c-Jun/TAM-67 [10]; Figure 1d, lanes 7–9) which inhibits changes in shape and motility induced by Fos [9]. Additionally, Fos-transformed Rat-1 cells showed a marked increase in colocalization of ezrin with F-actin, which is concentrated in plasma membrane ruffles at the tips of long filamentous

Figure 1

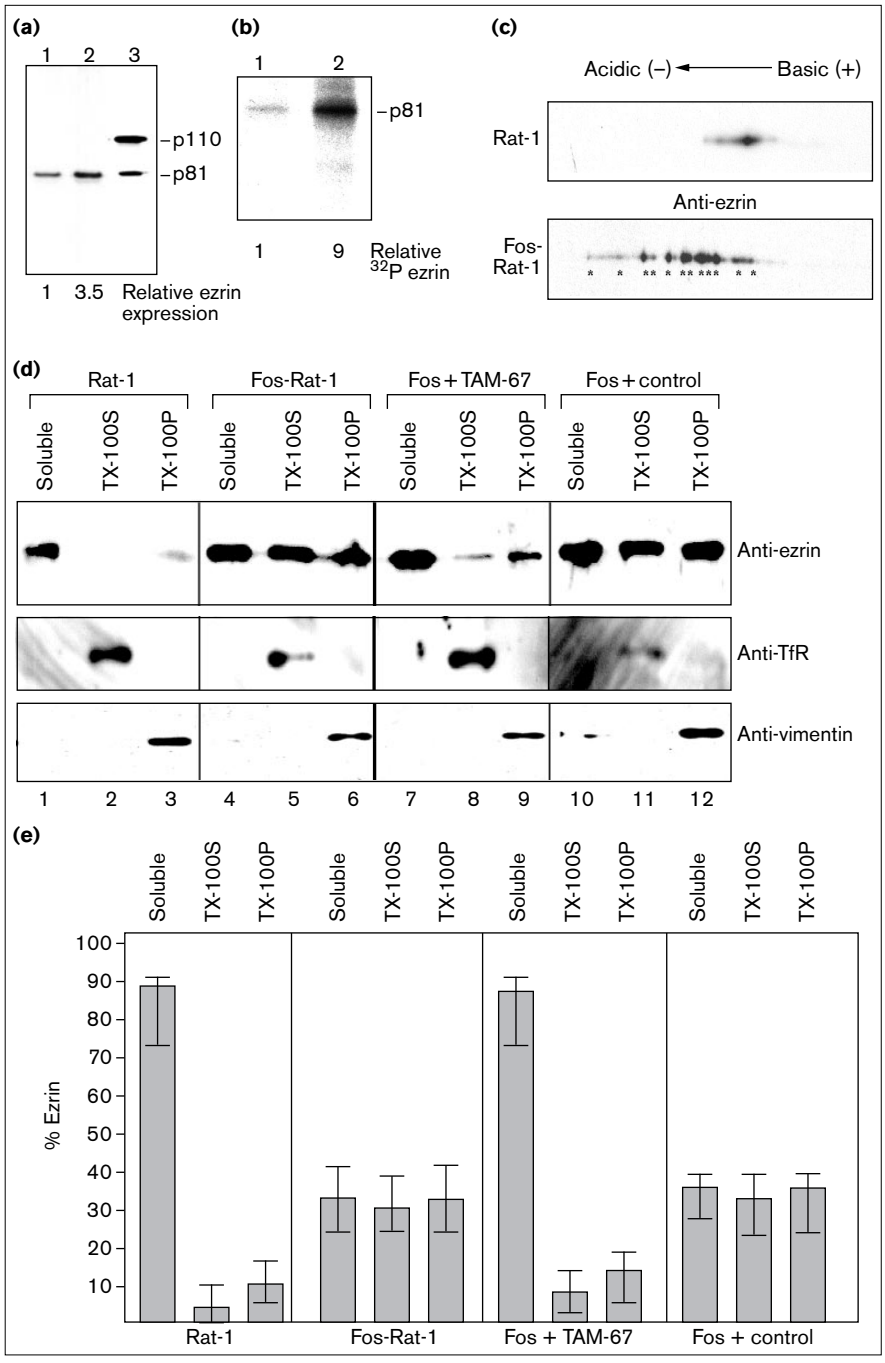

Biochemical analysis of ezrin in normal and Fos-transformed Rat-1 cells. **(a)** Immunoprecipitation of p81 ezrin with anti-ezrin IgG used for CALI; Rat-1 cells (lane 1), Fos-transformed Rat-1 cells (lane 2), and Fos-transformed Rat-1 cells transiently transfected with ezrin–GFP (p110, lane 3). Quantitation revealed that there was a 3–4-fold induction of ezrin in Fos-transformed Rat-1 cells in comparison to wild-type Rat-1 cells. **(b)** Immunoprecipitation of ^{32}P-labelled ezrin from Rat-1 cells (lane 1) or Fos-transformed Rat-1 cells (lane 2). Quantitation revealed that there was an 8–9-fold increase in phosphorylation of ezrin in Fos-transformed Rat-1 cells in comparison to wild-type Rat-1 cells. **(c)** Two-dimensional SDS–PAGE immunoblot of ezrin from Rat-1 cell lysates (upper panel) and Fos-transformed Rat-1 cell lysates (lower panel). Asterisks indicate the abundant phosphorylated ezrin isoforms in Fos-transformed Rat-1 cells. **(d)** Immunoblot of cell fractions representing soluble, Triton X-100 soluble (TX-100S) and Triton X-100 insoluble (TX-100P) material from Rat-1 cells (lanes 1–3), Fos-transformed Rat-1 cells (lanes 4–6) and Fos-transformed Rat-1 cells expressing TAM-67 (Fos + TAM-67, lanes 7–9) or control vector (Fos + Control, lanes 10–12) probed for ezrin expression with an anti-ezrin antibody. The blot was also probed with anti-transferrin receptor (anti-TfR) and anti-vimentin antibodies to ensure enrichment for Triton X-100 soluble and cytoskeletal components, respectively, in the appropriate cell fractions. **(e)** Quantitation of (d). Ezrin from each cell fraction is expressed as a percentage of all fractions, $n = 3$.

cell processes (pseudopodia; Figure 2b, arrowheads) and in microvilli. In normal Rat-1 cells, the majority of ezrin immunostaining was cytosolic and did not colocalize with F-actin (Figure 2a).

Ezrin is associated with motile leading-edge structures in Fos-transformed Rat-1 fibroblasts

The immunocytochemical data was confirmed by observing the dynamic cellular distribution of a fusion protein consisting of green fluorescent protein (GFP) [11] fused to the carboxy terminus of ezrin, creating ezrin–GFP (Figure 1a, lane 3). The distribution of ezrin–GFP was indistinguishable immunocytochemically from that of endogenous ezrin and colocalized with F-actin in plasma membrane ruffles at the tips of pseudopodia (Figure 3b, arrowheads), and in microvilli in Fos-transformed Rat-1 cells; in normal Rat-1 cells, ezrin–GFP was predominantly cytosolic (Figure 3a). Time-lapse video fluorescence microscopy of

Figure 2

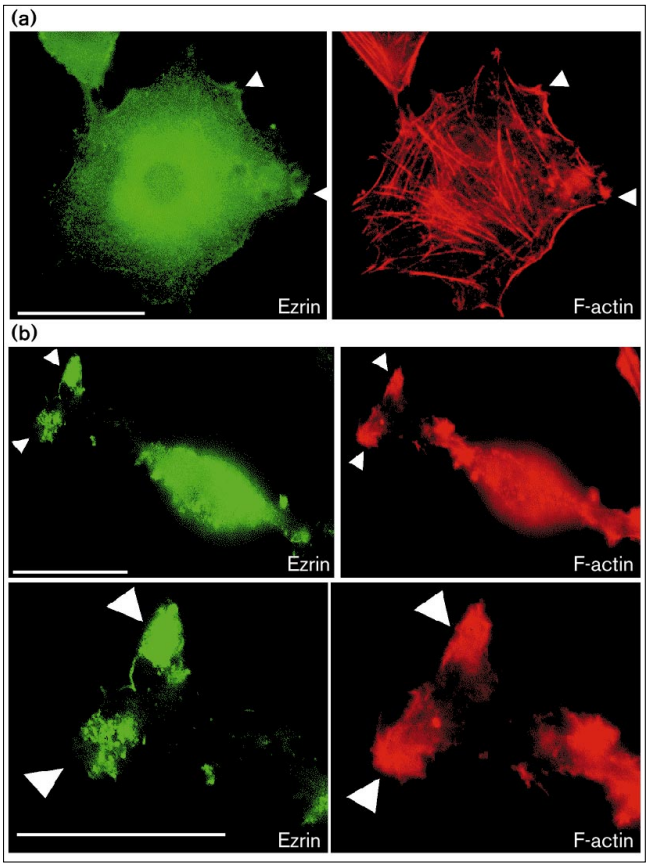

Double immunofluorescence of ezrin and F-actin in **(a)** Rat-1 cells and **(b)** Fos-transformed Rat-1 cells. The arrowheads in (a) indicate the minor colocalization of ezrin and F-actin at peripheral membrane ruffles and, in (b), the major colocalization of the proteins at membrane ruffles of pseudopodial tips. The lower panels in (b) show an enlarged micrograph of ezrin and F-actin colocalization at leading-edge plasma-membrane ruffles of Fos-transformed Rat-1cells. Scale bar = 25 μm.

ezrin–GFP revealed that a pool of fluorescence was consistently associated with the plasma membrane at the membrane-ruffling area of the tips of extending pseudopodia in Fos-transformed Rat-1 cells (Figure 3d, arrowheads). Although this fluorescence was primarily diffuse in normal Rat-1 cells (Figure 3c), a minor pool of ezrin–GFP was associated with dynamic phase-dark structures around the cell periphery (Figure 3c, arrowheads).

Ablation of ezrin by micro-CALI

To test whether ezrin functions in pseudopodial motility in Fos-transformed Rat-1 cells, we specifically ablated the dynamic ezrin pool present in leading lamellae using micro-CALI (chromophore-assisted laser irradiation; [12–14]). This technique inactivates proteins *in vivo* using microinjected non-blocking antibodies conjugated to a chromophore (malachite green, MG): upon absorption of 620 nm laser light, hydroxyl radicals are released which then inactivate antibody-bound protein. To confirm that CALI could inhibit the biochemical activity of ezrin, we used a solid-phase assay that monitored the binding of F-actin to recombinant ezrin coated on 96-well chambers [15]. Laser irradiation selectively inhibited actin binding in chambers treated with MG-conjugated anti-ezrin antibody, but not in chambers treated with control MG-conjugated immunoglobulin G (IgG) antibody (Figure 4a, lanes 2,4) indicating that *in vitro* CALI can inhibit the binding of ezrin to F-actin. The anti-ezrin antibody used was monospecific for ezrin as shown by the immunoprecipitation of a single 81 kDa species from ^{35}S-labelled cell lysates from Rat-1 or Fos-transformed Rat-1 cells (Figure 1a, lanes 1,2) and by specific recognition of ezrin by western blotting analysis of ERM proteins produced in baculovirally infected Sf9 insect cells (Figure 4b). Microinjection of the MG–anti-ezrin antibody produced a similar staining pattern to that revealed by immunocytochemistry (Figure 4c,d, arrowheads). Injection of the antibody without laser irradiation caused no obvious effect on plasma membrane ruffling or cell shape, because these cells resembled those that had been microinjected with non-immune MG–IgG (Figure 5a–d and Table 1).

Micro-CALI of ezrin in single Fos-transformed fibroblasts at the extending leading edge of the cell resulted in a rapid, reversible loss of pre-existing plasma-membrane ruffles and the inhibition of further membrane ruffling. Inhibition of plasma membrane ruffling began within the 5 minute period of irradiation (Figure 5a) before recovery of peripheral ruffling and plasma membrane extension after 10–15 minutes (data not shown). In Fos-transformed Rat-1 cells, the inhibition of plasma-membrane ruffling was accompanied by a net retraction of pseudopodia (Figure 5a, and Table 1, $p < 0.001$). No significant effect on plasma-membrane ruffling or extension of pseudo podia was observed following micro-CALI irradiation of Fos-transformed Rat-1 fibroblasts microinjected with control non-immune MG–IgG (Figure 5b, Table 1, $p > 0.05$).

To investigate the role of ezrin in normal Rat-1 cells, where it is found mainly in the cytosol, we selectively irradiated the cell body, avoiding irradiation at the leading edge. Micro-CALI after microinjection of MG-labeled anti-ezrin (Figure 5c), but not non-immune MG–IgG (Figure 5d), resulted in a pronounced loss of shape and rounding of the cell, characterized by a shearing at the cell periphery leaving peripheral material and filamentous structures attached to the substratum (Figure 5c, arrowheads and inset). No obvious effect on cell shape was observed after similar laser irradiation of the cell body in Fos-transformed Rat-1 cells (data not shown). These findings suggest that ezrin might have distinct roles depending on its subcellular association.

Figure 3

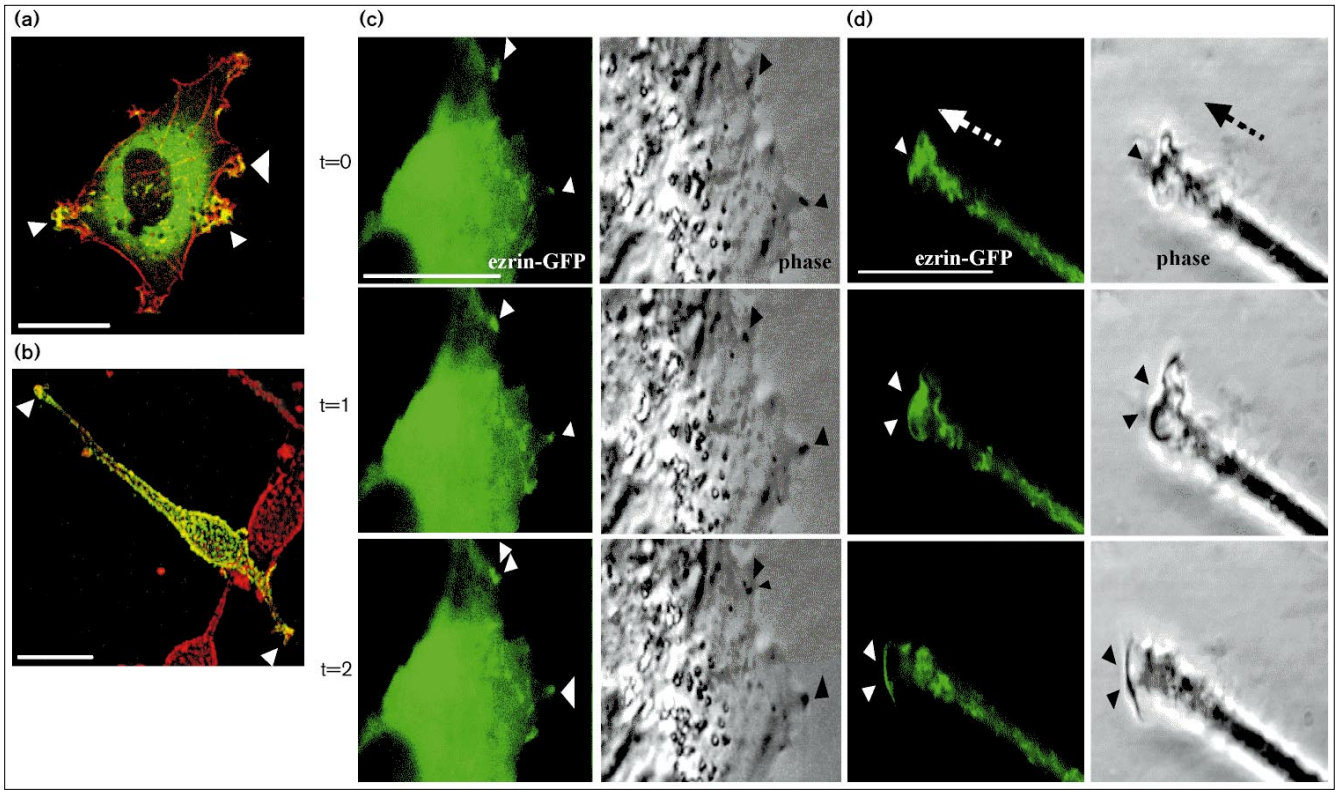

Localization and dynamics of ezrin–GFP. Merged immunofluoresence micrographs of ezrin–GFP (green) and F-actin (red) in **(a)** Rat-1 cells and **(b)** Fos-transformed Rat-1 cells. The arrowheads in (a) indicate the colocalization of ezrin–GFP and F-actin at peripheral membrane ruffles, and, in (b), the colocalization of the proteins at membrane ruffles of pseudopodial tips. Fluorescence time-lapse microscopy of **(c)** a wild-type Rat-1 cell, showing diffuse fluorescence with minor concentration of ezrin–GFP in dynamic peripheral structures (arrowheads) and **(d)** a Fos-transformed Rat-1 cell, showing concentration of ezrin–GFP at the plasma membrane (arrowheads) of the extending leading edge (dotted arrows). Experiments are representative of variable expression levels of transfected ezrin–GFP. Time is shown in minutes; scale bar = 25 μm.

Discussion

Few proteins associated with the cytoskeleton have been shown to mediate the shape and locomotory changes characteristic of oncogene transformation [16]. The increased expression [4], hyperphosphorylation, and subcellular redistribution of ezrin upon fibroblast transformation coupled with its role is cell shape and motility in these cells suggest that ezrin is important for these changes that occur during oncogenic transformation. Consistent with this proposal is the concomitant AP-1-mediated increase in expression of the hyaluronan receptor CD44, a resident plasma membrane ligand for ERM proteins [7], during cell transformation and invasion [9]. Moreover, the interaction between CD44 and ERM proteins might be regulated by the small GTPase Rho [17], which is also necessary for oncogenic transformation [18] and involved in controlling the actin cytoskeleton [19].

Antisense and overexpression studies with ERM family proteins have indicated both distinct and redundant functions for ERM proteins in plasma-membrane protrusion, substrate adhesion and the generation of cell-surface microvilli [2,3,20–22]. The ERM proteins may also compete for binding to a common plasma-membrane protein [23]. It is likely that the acute nature of the loss-of-function damage imposed by micro-CALI precludes redundancy through the compensatory effects of other ERM proteins [14], thereby allowing an unambiguous definition of ezrin function. A small measure of micro-CALI-induced damage may occur to radixin or moesin, if these proteins interact with and closely contact ezrin, as has been reported [24,25]; however, we believe this to be unlikely because the damage caused by CALI is spatially specific even between subunits of a small protein complex [26].

Conclusions

Our findings indicate that ezrin plays an important role in plasma membrane ruffling in Fos-transformed fibroblasts and that this function is required for the extension of pseudopodia, the filamentous cell processes typical of transformation. We suggest that putative ezrin kinases active in

Figure 4

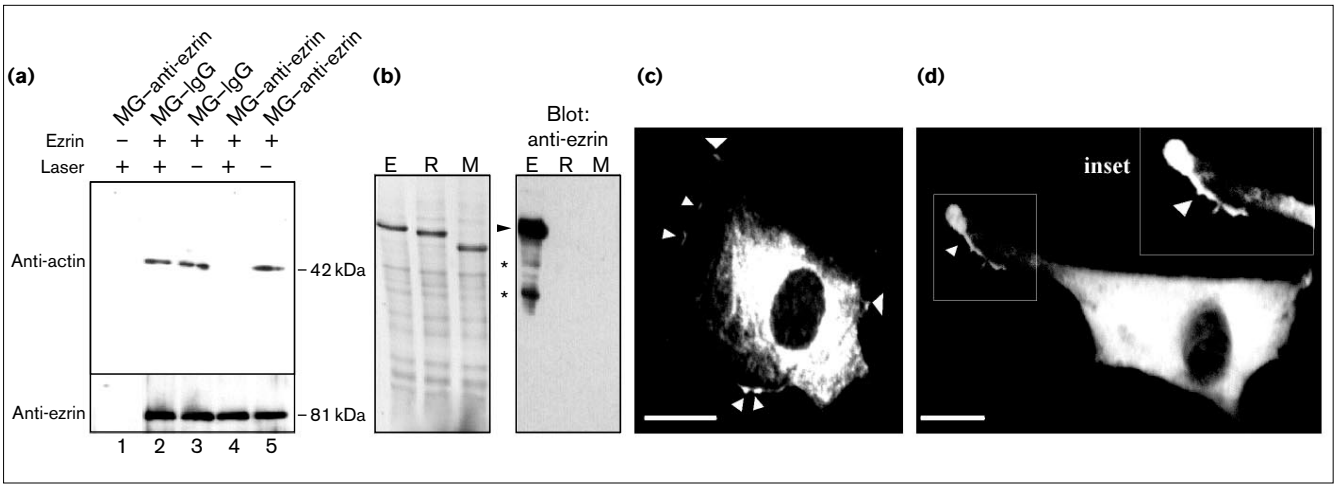

Ablation of ezrin by CALI. **(a)** Immunoblot of F-actin (anti-actin, upper panel) bound to recombinant ezrin (anti-ezrin, lower panel) in a solid-phase assay after *in vitro* CALI. Lane 1, no ezrin, MG–anti-ezrin, laser irradiation; lane 2, MG–IgG, laser irradiation; lane 3, MG–IgG, no laser irradiation; lane 4, MG–anti-ezrin, laser irradiation; lane 5, MG–anti-ezrin, no laser irradiation. **(b)** Specific recognition of ezrin by anti-ezrin IgG. The left panel shows a Coomassie-blue-stained gel of total Sf9 lysates from cells infected with baculoviruses producing ezrin (E), radixin (R) or moesin (M). The right panel shows the western blot analysis of baculovirally produced ERM proteins probed with anti-ezrin IgG. The arrowhead indicates reactivity with ezrin. A long exposure is shown revealing the presence of minor ezrin breakdown products in the Sf9 lysates (arterisks), but no cross-reactivity to either radixin or moesin. Binding of microinjected MG–anti-ezrin IgG in **(c)** Rat-1cells and **(d)** Fos-transformed Rat-1 cells. Specific binding was observed in peripheral plasma-membrane ruffles in Rat-1 cells (arrowheads in c) and at the leading edge in Fos-transformed Rat-1 cells (arrowhead in d), in addition to general cytosolic staining some of which represents non-specific retention of antibody after fixation. The inset in (d) shows a higher magnification of the leading edge of a Fos-transformed Rat-1 cell showing binding of MG–anti-ezrin antibody (arrowhead).

Figure 5

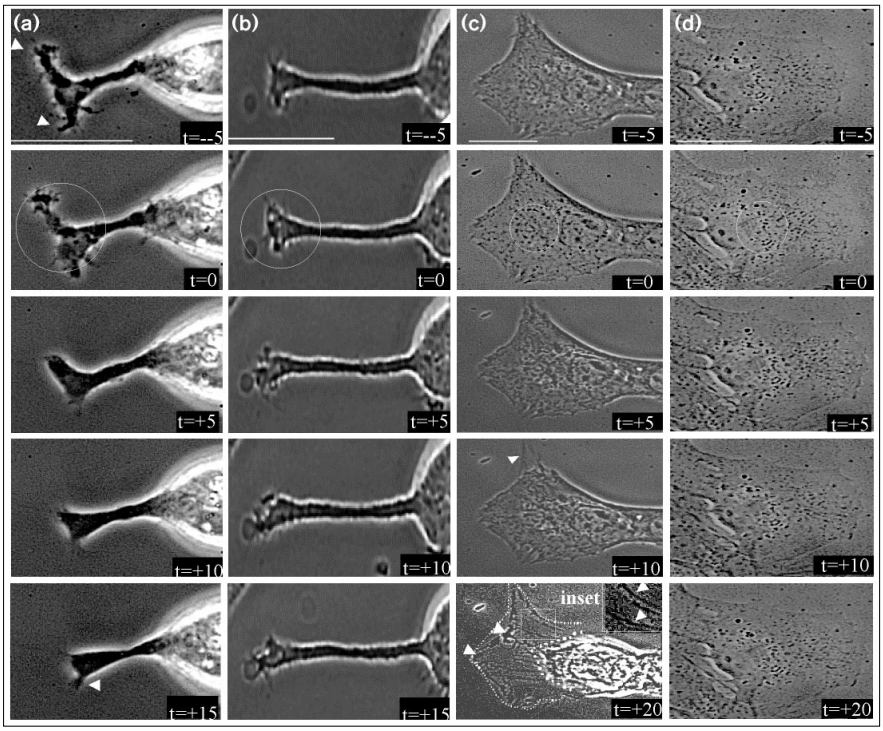

Micro-CALI *in vivo*. Phase time-lapse images of micro-CALI at **(a,b)** pseudopodial extensions of Fos-transformed Rat-1 cells or **(c,d)** in the cell body of Rat-1 cells after microinjection with MG-labelled anti-ezrin (a,c) or non-immune IgG (b,d). A rapid inhibition of membrane ruffling is shown in (a) and indicated by the arrowheads in t = –5, prior to irradiation, at the leading edge beginning during the period of laser irradiation (t = +5) and persisting for 10–15 min. The arrowhead in (a) at t = +15 indicates that there is some recovery of plasma membrane extension. (c) In Rat-1 cells, micro-CALI outside the cell periphery resulted in the loss of cell architecture, beginning 5–10 min after micro-CALI with deposition of peripheral material (arrowheads in (c), t = +20) and filaments (arrowheads in the inset) on the substratum followed by cell rounding (t = +20). Also shown is the outline of the cell before (fine dotted line) and after (thick dotted line) micro-CALI. Time is shown in min, –5 = prior to irradiation, +5 = after 5 min of laser irradiation. In (a–d), open circles = 10 μm diameter laser spot. Scale bar = 15 μm.

Fos-transformed Rat-1 fibroblasts might serve to unmask a cryptic F-actin-dependent extension activity analogous to that seen upon overexpression of an amino-terminally truncated ezrin protein [21]. In Rat-1 cells, inactivation of the cytosolic ezrin pool suggests that, despite its apparent absence from focal adhesions [27], ezrin is required to maintain cell shape. We suggest that a dynamic association of cytosolic ezrin with F-actin and/or plasma-membrane ligands might play a role in the initiation of new focal adhesions, rather than a role in the maintenance of focal adhesion structure. In accord with such a proposal, another ERM protein, moesin, has recently been shown to induce the formation of integrin-containing focal complexes and adhesions in quiescent Swiss 3T3 fibroblasts [28]. Inactivation of cytosolic ezrin could prevent the initiation of new focal adhesions, thereby rendering cell shape subject to perturbation by tension during motility. Loss of adhesion/cell rounding in Rat-1 cells resulting from the depletion of cytosolic ezrin by micro-CALI, is also a hallmark of cell transformation [1]. We suggest that a similar depletion of cytosolic ezrin by hyperphosphorylation and association with the plasma membrane or cytoskeleton might occur during Fos-induced cell transformation.

Materials and methods

Metabolic labelling, immunoprecipitation

For metabolic labelling with [^{35}S]-cysteine/methionine or inorganic ^{32}P, Rat-1 cells (208F clone) or Rat-1 cells virally transduced by the Finkel-Biskis-Reilly (FBR) v-*fos* oncogene were labelled in the exponential phase of growth with 100 μCi/ml ^{35}S-Promix, or 1 mCi/ml inorganic ^{32}P, (Amersham) for 4 h in DMEM/5%FCS lacking cysteine and methionine (for ^{35}S-labelling) or for 1 h in phosphate-free DMEM/5%FCS (for ^{32}P-labelling) and lysed in RIPA buffer (150 mM NaCl, 1% NP-40, 0.5% sodium deoxycholate, 0.1% SDS, 50 mM Tris pH8.0) containing 1 mM Na_3VO_4, 1 mM PMSF, 5 mM NaF, 1 mM β-glycerophosphate and 1 μg/ml okadaic acid. Lysates containing 400 μg of protein were immunoprecipitated for 60 min on ice with anti-ezrin IgG and immune complexes were collected with protein-A–sepharose. Immunoprecipitates analysed by 10% SDS–PAGE and dried gels were exposed to Kodak X-OMAT film. Autoradiographic quantitation of the amount of ezrin immunoprecipitated from Rat-1 cells or Fos-transformed Rat-1 cells or of ^{32}P-labelled ezrin was performed with Quantity-One software (PDI).

Two-dimensional SDS–PAGE, cell fractionation analysis

For analysis by two-dimensional SDS–PAGE, cells were lysed in two-dimensional sample buffer (10 M urea, 4% NP-40, 5.5% ampholytes pH3-10/2D-optimised (Millipore), 100 mM DTT, 0.003% BPB, 1 mM Na_3VO_4, 1 mM PMSF, 5 mM NaF, 1 mM β-glycerophosphate and 1 μg/ml okadaic acid), two-dimensional SDS–PAGE carried out according to [29], and the gels were transferred to Immobilon P membranes. Immunoblots were probed with anti-ezrin sera (1:10 000) and processed and developed using the enhanced chemiluminescence system (Amersham). A similar induction of ezrin expression and phosphorylation was also observed after conditional transformation of Rat-1 cells by a c-Fos–ER fusion protein (data not shown). For fractionation analysis, cells were homogenized in 10 mM Hepes pH 7.4, 1 mM Na_3VO_4, 2.5 mM $MgCl_2$, 1 mM EGTA, 10% glycerol, 100 μg/ml CHAPS, 1 mM PMSF, and protease inhibitors (Complete, BCL) were centrifuged (20 min, 18 000 r.p.m.), soluble material removed, and the pellet homogenized in Triton X-100 lysis buffer (25 mM MES pH 6.4, 1 mM Na_3VO_4, 2.5 mM $MgCl_2$, 3 mM EGTA, 0.5% Triton X- 100, 10% glycerol, 1 mM PMSF, and protease inhibitors (Complete, BCL). Triton X-100-soluble material was removed following centrifugation (4^{0}C for 20 min at 14 000 r.p.m.) and the remaining insoluble pellet solubilized by sonication in SDS sample buffer. Proteins (10 μg) in each cell fraction were adjusted to 1 × sample buffer, subjected to 10% SDS–PAGE and transferred to Immobilon-P membranes (Millipore). Immunoblots were probed with anti-ezrin (1:10 000), anti-transferrin receptor H68.4 (1:1000) and anti-vimentin (Sigma) antibodies. Autoradiographic quantitation was performed using Quantity-One software (PDI) and represents the mean of three separate experiments.

Immunofluorescence

Immunofluorescence was performed on a Nikon Diaphot microscope equipped with ultraviolet illumination. Anti-ezrin IgG (1:300) and TRITC–phalloidin (1 μg/ml, Sigma) were used. FITC-labelled anti-rabbit IgG (1:100, Jackson Immunoresearch) was used to detect bound ezrin antibody. Cells plated on coverslips were fixed for 15 min at 37°C in 4% paraformaldehyde, washed extensively in PBS and permeabilized in PBS/20 mM glycine/0.05% TX-100 for 5 min. Blocking of nonspecific binding was performed for 20 min in blocking buffer (PBS/0.5% BSA (Fraction V, Sigma)/10% FCS) before incubation for 60 min at room temperature in the same buffer containing anti-ezrin IgG. After extensive washing in blocking buffer, cells were incubated in blocking buffer containing secondary antibody and TRITC-phalloidin for 45 min, washed extensively in PBS and mounted (Vectashield, Vector Laboratories). Cells were imaged with a 100× objective (Nikon PlanApo 100) and photographed under ultraviolet light on Ectachrome Elite 100 colour film using filter blocks for TRITC and FITC.

Construction of ezrin–GFP and fluoresence time-lapse microscopy

Cells were plated on glass coverslips after transient transfection (Genepulser, Biorad) with 10 μg of a construct expressing a carboxy-terminally-tagged ezrin–GFP fusion protein. This fusion was generated by ligating an *Eco*RI–*Sal*I PCR-amplified (*Pfu* polymerase; Stratagene) ezrin cDNA into pEGP-N1 (Clontech) with the following primers: 5′ primer; 5′-ACGTGAATCCCCGAAAATGCCGAAACCAATCAAT-3′; 3′ primer; 5′-ACGTGTCGACGACAGGGCCTCGAACTCGTCGAT-3′, where the underlined sequences represent the *Eco*RI (5′ primer) and *Sal1* (3′ primer) restriction sites, generating the construct pEGFPN1ezGFP. After 24 h, transfected cells were fixed and stained with TRITC–phalloidin and projections of dual channels, green (GFP) and red (TRITC–phalloidin) converted to TIFF images as above, or coverslips mounted on an MRC 600 Nikon Diaphot confocal laser microscope at 37°C in HEPES-buffered DMEM/10% FCS for fluorescence time-lapse microscopy. Dual phase and GFP signals at 30 sec intervals were collected with a COMOS programme (Biorad) and processed as TIFF images.

Table 1

Summary of micro-CALI data: quantitative change in pseudopodial extension in Fos-transformed Rat-1 fibroblasts

Condition	MG–anti-ezrin	MG–IgG
	Average change in pseudopodial length (μm ± s.e.m.)	
before CALI	+2.01 ± 0.45	+1.85 ± 0.33
after CALI	−3.63 ± 1.08*	+2.02 ± 0.35
n	15	12
retraction	12/15	1/12

Measurements of change in pseudopodial length of Fos-transformed Rat-1 captured as described [13] in the 10 min before and 10 min after laser irradiation. Data are shown as means ± SEM. *$p < 0.001$ following irradiation of MG–anti-ezrin-microinjected Fos-transformed Rat-1 by analysis of Student's unpaired *t*-test. The differences between other groups are not statistically significant by this test ($p > 0.05$).

In vitro *actin-binding assay*

The *in vitro* F-actin-binding assay [15] used 0.2 μg recombinant ezrin coated on 96-well needle-point chambers. Non-immune IgG or anti-ezrin IgG [30] (2 μg), labelled with malachite green (MG) to similar ratios (5–9 dyes per IgG molecule, [12]) were added to ezrin-coated or uncoated chambers in binding buffer lacking F-actin for 1 h at room temperature. Chambers were washed extensively in binding buffer, irradiated as described [12], and F-actin added in binding buffer. Bound F-actin and ezrin were eluted from the chambers in SDS–sample buffer and subjected to 10% SDS–PAGE. Duplicate immunoblots were probed with anti-actin monoclonal antibody (1:100, Sigma) or anti-ezrin sera (1:10 000).

Production of ERMs in baculovirally-infected Sf9 cells and microinjection

ERMs were produced in baculovirally-infected Sf9 cells as described [21]. Lysates were subjected to SDS–PAGE, stained with Coomassie blue or transferred to Immobilon P membranes and immunoblotted with anti-ezrin IgG and processed using the ECL system (Amersham). TRITC-labelled anti-rabbit IgG (1:100, Sigma) was used for microinjection of MG-labelled anti-ezrin IgG (5 μg/ml) and immunofluoresence to detect bound ezrin IgG.

Micro-CALI

Fos-transformed Rat-1 cells or Rat-1 cells, microinjected at a concentration of 1 mg/ml with MG-labelled antibodies and fluorescein-dextran (3 mg/ml, Molecular Probes) were localized after 60–90 min by epifluorescence and subjected to micro-CALI. Fos-transformed Rat-1 cells were viewed for 10–15 min with a Nikon Diaphot microscope with phase-contrast optics to determine the direction of cell locomotion prior to micro-CALI irradiation. Time-lapse images (one frame every 30 sec) and image enhancements were facilitated by custom-written software [13]. Micro-CALI (10 μm diameter laser spot) was performed for 5 min, followed by an additional 20–180 min observation period.

Acknowledgements

We thank M. Martin for construction of recombinant ERM baculovirus constructs and production of ERMs using baculovirally-infected Sf9 cells and M. Arpin and G. Thomas for radixin and moesin cDNAs used for construction of recombinant baculoviruses. We also thank A. Hall, L. Castelo, and C. Isacke for discussion; C. Isacke for providing a monoclonal antibody to the transferrin receptor; and J.A. Wyke for support and critical reading of the manuscript. R.F.L. is also indebted to Peter McHardy for photographic assistance and F-S. Wang for advice with micro-CALI. Supported by a U.I.C.C. technology transfer fellowship (to R.F.L) and grants from the Medical Research Council (to R.F.L), the Cancer Research Campaign (to B.W.O), the Association Pour La Research Sur Le Cancer, Ligue Nationale Contre Le Cancer and European Commision (to P.M and C.R), CNRS Cell Biology Project 96033 (to C.R.) an NIH NRSA (to C.S.) and the N.I.H grant and Klingenstein Fellowship (to D.G.J).

References

1. Bershadsky AD, Vasiliev JM: *Cytoskeleton*. New York: Plenum Press; 1983.
2. Berryman M, Gary R, Bretscher A: **Ezrin oligomers are major cytoskeletal components of placental microvilli: a proposal for their involvement in cortical morphogenesis.** *J Cell Biol* 1995, **131:**1231-1242.
3. Tsukita S, Yonemura S, Tsukita SH: **ERM (ezrin/radixin/moesin) family: from cytoskeleton to signal transduction.** *Curr Opin Cell Biol* 1997, **9:**70-75.
4. Joos KU, Muller R: **Deregulation of genes encoding microfilament-associated proteins during Fos-induced morphological transformation.** *Oncogene* 1995, **10:**603-608.
5. Lloyd A, Yancheva N, Wasylyk B: **Transformation suppressor activity of a Jun transcription factor lacking its activation domain.** *Nature* 1991, **352:**635-638.
6. Johnson R, Spiegelman B, Hanahan D, Wisdom R: **Cellular transformation and malignancy induced by *ras* require c-*jun*.** *Mol Cell Biol* 1996, **16:**4504-4511.
7. Tsukita SH, Oishi K, Sato N, Sagara J, Kawai A, Tsukita S: **ERM family members as molecular linkers between the cell-surface glycoprotein CD44 and actin-based cytoskeletons.** *J Cell Biol* 1994, **126:**391-401.
8. Hennigan RF, Hawker KL, Ozanne BW: **Fos-transformation genes associated with invasion.** *Oncogene* 1994, **9:**3591-3600.
9. Lamb RF, Hennigan RF, Turnbull K, Katsanakis KD, MacKenzie ED, Birnie GD, Ozanne BW: **AP-1-mediated invasion requires increased expression of the hyaluronan receptor CD44.** *Mol Cell Biol* 1997, **17:**963-976.
10. Brown PH, Chen TK, Birrer MJ: **Mechanism of action of a dominant-negative c-*jun*.** *Oncogene* 1994, **9:**791-799.
11. Heim R, Cubitt AB, Tsien RY: **Improved green fluorescence.** *Nature* 1995, **373:**663-664.
12. Chang HY, Takei K, Sydor A, Born T, Rusnak F, Jay DG: **Asymmetric retraction of growth cone filopodia following focal inactivation of calcineurin.** *Nature* 1995, **376:**686-690.
13. Wang F-S, Wolenski JS, Cheney RE, Mooseker MS, Jay DG: **Function of myosin-V in filopodial extension of neuronal growth cones.** *Science* 1996, **273:**660-603.
14. Wang F-S, Jay DG: **Chromophore-assisted laser inactivation (CALI): probing protein function *in situ* with a high degree of spatial and temporal resolution.** *Trends Cell Biol* 1996, **6:**442-445.
15. Roy C, Martin M, Mangeat P: **A dual involvement of the amino-terminal domain of ezrin in F- and G-actin binding.** *J Biol Chem* 1997, in press.
16. Parsons JT, Parsons SJ: **Src family protein tyrosine kinases: cooperating with growth factor and adhesion signaling pathways.** *Curr Opin Cell Biol* 1997, **9:**187-192.
17. Hirao M, Sato N, Kondo T, Yonemura S, Monden M, Sasaki T, *et al.*: **Regulation mechanism of ERM (ezrin/radixin/moesin) protein/plasma membrane association: possible involvement of phosphatidylinositol turnover and Rho-dependent signalling pathway.** *J Cell Biol* 1996, **135:**37-51.
18. Qui R-G, Chen J, McCormick F, Symons M: **A role for Rho in Ras transformation.** *Proc Natl Acad Sci USA* 1995, **92:**11781-11785.
19. Ridley AJ, Hall A: **The small GTP-binding protein Rho regulates the assembly of focal adhesions and actin stress fibres in response to growth factors.** *Cell* 1992, **70:**389-399.
20. Takeuchi K, Sato N, Kasahara H, Funayama N, Nagafuchi A, Yonemura S, *et al.*: **Perturbation of cell adhesion and microvilli formation by antisense oligonucleotides to ERM family members.** *J Cell Biol* 1994, **125:**1371-1384.
21. Martin M, Andreoli C, Sahuquet A, Montcorrier P, Algrain M, Mangeat P: **Ezrin NH2-terminal domain inhibits the cell extension activity of the COOH-terminal domain.** *J Cell Biol* 1995, **128:**1081-1093.
22. Helander TS, Carpen O, Turunen O, Kovanen PE, Vaheri A, Timonen T: **ICAM-2 redistributed by ezrin as a target for killer cells.** *Nature* 1996, **382:**265-268.
23. Henry MD, Agosti CG, Solomon F: **Molecular dissection of radixin: distinct and interdependent functions of the amino- and carboxy-terminal domains.** *J Cell Biol* 1995, **129:**1007-1022.
24. Gary R, Bretscher A: **Heterotypic and homotypic associations between ezrin and moesin, two putative membrane-cytoskeletal linking proteins.** *Proc Natl Acad Sci USA* 1993, **90:**10846-10850.
25. Gary R, Bretscher A: **Ezrin self-association involves binding of an N-terminal domain to a normally masked C-terminal domain that includes the F-actin binding site.** *Mol Biol Cell* 1995, **6:**1061-1075.
26. Liao JC, Berg LJ, Jay DG: **Chromophore-assisted laser inactivation of subunits of the T-cell receptor in living cells is spatially restricted.** *Photochem Photobiol* 1995, **62:**923-929.
27. Franck Z, Gary R, Bretscher A: **Moesin, like ezrin, colocalizes with actin in the cortical cytoskeleton in cultured cells, but its expression is more variable.** *J Cell Sci* 1993, **105:**219-231.
28. McKay DJG, Esch F, Furthmayr H, Hall A: **Rho- and Rac-dependent assembly of focal adhesion complexes and actin filaments in permeabilized cells: an essential role for ERM proteins.** *J Cell Biol* 1997, in press.
29. Garrels JI: **Quantitative two-dimentional gel electrophoresis of proteins.** *Methods Enzymol* 1983, **100:**411-424.
30. Andreoli C, Martin M, Le Borgne R, Reggio H, Mangeat P: **Ezrin has properties to self-assemble at the plasma membrane.** *J Cell Sci* 1994, **107:**2509-2521.

Because *Current Biology* operates a 'Continuous Publication System' for Research Papers, this paper has been published on the internet before being printed. The paper can be accessed from http://biomednet.com/cbiology/cub – for further information, see the explanation on the contents page.